AMERICAN SOCIETY FOR MICROBIOLOGY | Journal of Bacteriology®

MINIREVIEW

Seeing and Touching the Mycomembrane at the Nanoscale

Albertus Viljoen,[a] Esther Räth,[b] John D. Mckinney,[c] Georg E. Fantner,[b] Yves F. Dufrêne[a,d]

[a]Louvain Institute of Biomolecular Science and Technology, UCLouvain, Louvain-la-Neuve, Belgium
[b]School of Engineering, Swiss Federal Institute of Technology (EPFL), Lausanne, Switzerland
[c]School of Life Sciences, Swiss Federal Institute of Technology (EPFL), Lausanne, Switzerland
[d]Walloon Excellence in Life Sciences and Biotechnology (WELBIO), Wavre, Belgium

Albertus Viljoen and Esther Räth contributed equally to this work. Author order was determined by drawing straws.

ABSTRACT Mycobacteria have unique cell envelopes, surface properties, and growth dynamics, which all play a part in the ability of these important pathogens to infect, evade host immunity, disseminate, and resist antibiotic challenges. Recent atomic force microscopy (AFM) studies have brought new insights into the nanometer-scale ultrastructural, adhesive, and mechanical properties of mycobacteria. The molecular forces with which mycobacterial adhesins bind to host factors, like heparin and fibronectin, and the hydrophobic properties of the mycomembrane have been unraveled by AFM force spectroscopy studies. Real-time correlative AFM and fluorescence imaging have delineated a complex interplay between surface ultrastructure, tensile stresses within the cell envelope, and cellular processes leading to division. The unique capabilities of AFM, which include subdiffraction-limit topographic imaging and piconewton force sensitivity, have great potential to resolve important questions that remain unanswered on the molecular interactions, surface properties, and growth dynamics of this important class of pathogens.

KEYWORDS mycobacterial envelope, ultrastructure, adhesins, binding force, chemical properties, growth dynamics, drugs, atomic force microscopy

THE MYCOMEMBRANE: FROM THE CELL SURFACE TO GROWTH DYNAMICS

Mycobacteria owe their pathogenicity and recalcitrance to antibiotics largely to their unique cell envelope (1). The mycobacterial cell envelope consists of a peptidoglycan (PG) layer bearing similarity to the PG of *Escherichia coli*, with a few minor differences (2). Distinctive to the *Corynebacteriaceae* family, from which the *Mycobacterium* genus stems, the PG is covalently linked to another large polysaccharide called arabinogalactan (AG). The ends of the arabinan portion of the AG are esterified with very large fatty acids (60 to 90 carbon chains) called mycolic acids forming the inner leaflet of the mycobacterial outer membrane, known as the mycomembrane. The outer leaflet of the mycomembrane consists of a large panoply of exotic, extractable lipids, some of them also containing mycolic acids. The mycomembrane, with its densely packed large fatty acids, is thus a consequential hydrophobic barrier to antibiotics and chemotherapeutic agents whose targets are periplasmic or cytosolic (1). Moreover, like the PG layer, the AG and mycolic acid layers are also essential to the survival and growth of all mycobacteria, and therefore the biosynthetic machinery of their components are excellent drug targets (*viz.*, the antitubercular ethambutol targets AG synthesis and isoniazid and ethionamide target mycolic acid synthesis).

The mycomembrane largely determines the physical and chemical properties of the mycobacterial cell surface, a structure that is at the interface between mycobacteria and their environment. Therefore, the physiology and mechanics of this structure fundamentally form a part of the bigger picture of mycobacterial pathophysiology. It is on

Citation Viljoen A, Räth E, Mckinney JD, Fantner GE, Dufrêne YF. 2021. Seeing and touching the mycomembrane at the nanoscale. J Bacteriol 203:e00547-20. https://doi.org/10.1128/JB.00547-20.

Editor William Margolin, McGovern Medical School

Copyright © 2021 American Society for Microbiology. All Rights Reserved.

Address correspondence to Georg E. Fantner, georg.fantner@epfl.ch, or Yves F. Dufrêne, yves.dufrene@uclouvain.be.

Accepted manuscript posted online 19 January 2021

Published 21 April 2021

the surface of the bacteria where hydrophobic lipids are exposed that drive their association with small water droplets, allowing their transmission by aerosols (3–5). It is also here where a large variety of lipids and saccharides interact with receptors on immune cells, where specialized adhesins bind to host extracellular matrix proteins (6–8), and where interbacterial interactions lead to the formation of mycobacterial cords (9, 10). New evidence even suggests that features in the ultrastructure of the mycobacterial cell surface predict growth and division events (11).

Not only is the structure of the mycobacterial cell envelope noncanonical, but the way it is synthesized during growth is also very different from model rod-shaped bacteria like *E. coli* and *Bacillus subtilis*, where new cell wall material is continuously inserted along the growing sidewalls of the cells (12). In mycobacteria, insertion of new cell wall material occurs mainly at the poles (13). In addition, asymmetric mycobacterial division and elongation underlie the occurrence of nascent cells with variable cell lengths, a factor that contributes to single-cell phenotypic heterogeneity (14). Mycobacteria, like other bacteria, rely on this phenotypic heterogeneity at the single-cell level to optimize survival of subpopulations of cells in diverse, often hostile microenvironments (for recent review on this topic, see reference 15).

Large questions regarding the surface properties of the mycomembrane include the following. How strong are the interactions between surface components like hydrophobic groups or adhesins and their binding partners? What are the nanoscale distributions of these components on the surface? How does the ultrastructure of the mycobacterial surface change as the bacteria grow and divide? How is phenotypic heterogeneity reflected in the ultrastructural and biophysical properties of the cells at the nanoscale? As a single-cell technique with subdiffraction limit resolution and force sensitivity, atomic force microscopy (AFM) has helped to address these questions.

AFM: FEELING THE FORCE

AFM functions by touching samples with a very sharp tip (probe) using a small amount of force (e.g., 100 pN) while raster scanning to obtain topographic images with *x-y* resolution that can range from ~50 nm on cells to less than a nanometer on model membranes (16). Different imaging modes of AFM exist, including correlative imaging with fluorescence microscopy (Fig. 1A) and gentle, fast, and dynamic modes allowing real-time visualization of single proteins performing their actions and undergoing conformational changes in two-dimensional (2D) crystals or in supported lipid bilayers (for more details, see references 17 to 19). But, AFM is also an ultrasensitive force-measuring device, an approach called force spectroscopy (Fig. 1B) (20). Here, force-distance curves are recorded by pushing the tip (often functionalized with chemical groups or bioligands) against the sample and then retracting it while monitoring force and the exact position of the tip at each point of its movement, enabling the investigation of physical properties and molecular interactions. These include cell wall mechanics (stiffness/elasticity/tensile strength), surface hydrophobicity, and the binding strength between receptors and their ligands. Furthermore, recording arrays of force-distance curves across the surface allows spatial mapping of these properties with nanoscale resolution (21, 22).

FUNCTIONAL ANALYSIS OF SINGLE ADHESINS

Bacterial pathogenesis is often initiated by the interaction between bacterial adhesins and specific ligands on the host cell surface (Fig. 2A). In the context of tuberculosis, evidence from *ex vivo* studies indicate that inhaled *Mycobacterium tuberculosis* bacilli adhere to epithelial cells lining alveoli, in a step that possibly precedes the infection of their preferred, but less abundant, macrophage host cells (23–26). At more advanced stages of disease, the bacilli disseminate into the host lymphatic system and bloodstream (27). In this process, the bacteria are exposed to physical shear forces, which they resist by adhering to extracellular matrix proteins (28). A variety of adhesins were identified that contribute to the ability of mycobacteria to bind to abiotic surfaces or

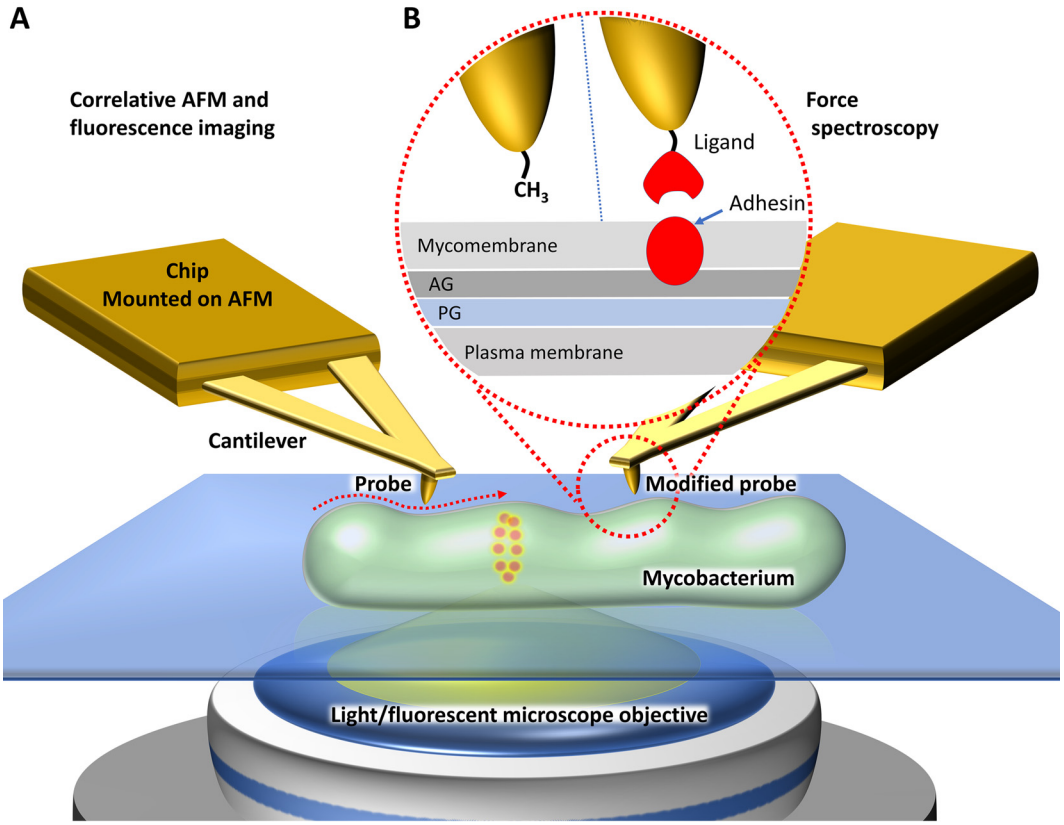

FIG 1 Two different basic AFM modes to study mycobacterial cells. (A) AFM imaging, in which the AFM probe is raster scanned across the sample, allows study of the nanoscale topography of cell walls along with correlative fluorescence microscopy imaging of cellular processes (e.g., markers of cellular division as illustrated by the fluorescent beads inside of the bacterium). (B) Force spectroscopy measurements with chemically (e.g., small molecules) or biologically sensitive (e.g., the ligand of an adhesin, such as human fibronectin) tips allows characterization of local physicochemical properties and of the strength of adhesin-ligand complexes.

to host extracellular matrix proteins (7, 8, 25, 26, 29). Pertinent questions are as follows: (i) what is the nanoscale distribution of adhesins on the bacterial surface, (ii) how strong are the interactions between the adhesins and their ligands, and (iii) what is the role of these interactions in cellular invasion (Fig. 2A)? AFM single-molecule force spectroscopy (SMFS) has proven a valuable tool to answer these questions. SMFS consists of using AFM tips modified with ligands to probe their cognate receptors (Fig. 1B), enabling the quantification of the molecular forces in these interactions and mapping the distribution of the receptors (e.g., single adhesins) on the surface of living bacteria (30).

The *M. tuberculosis* heparin-binding hemagglutinin (HBHA) surface adhesin works as a multifunctional adhesin. The C-terminal heparin-binding domain, containing several lysine-rich repeats, binds to heparan sulfate proteoglycan (HSPG) receptors on target epithelial cells (6, 31, 32), but HBHA can also form homodimers or homopolymers via an α-helical coiled-coil region in the N terminus of the protein (31). In addition, it was found that HBHA-coated latex beads could cross epithelial cell layers via transcytosis, which involved the reorganization of actin filaments in these cells (33). However, the strength and molecular mechanism of binding in these interactions were not unraveled. In a pioneering AFM study, the forces driving the interaction between HBHA and heparin sulfate proteoglycan (HSPG) receptors were captured by SMFS (34). AFM tips modified with single HBHA molecules were used to probe model surfaces coated with heparin, revealing that single electrostatic (lysine$^+$-SO_4^-) intermolecular bridges between the two binding partners resisted relatively weak forces of $\sim$50 pN. The data also showed that multiple such bridges form with increased contact time,

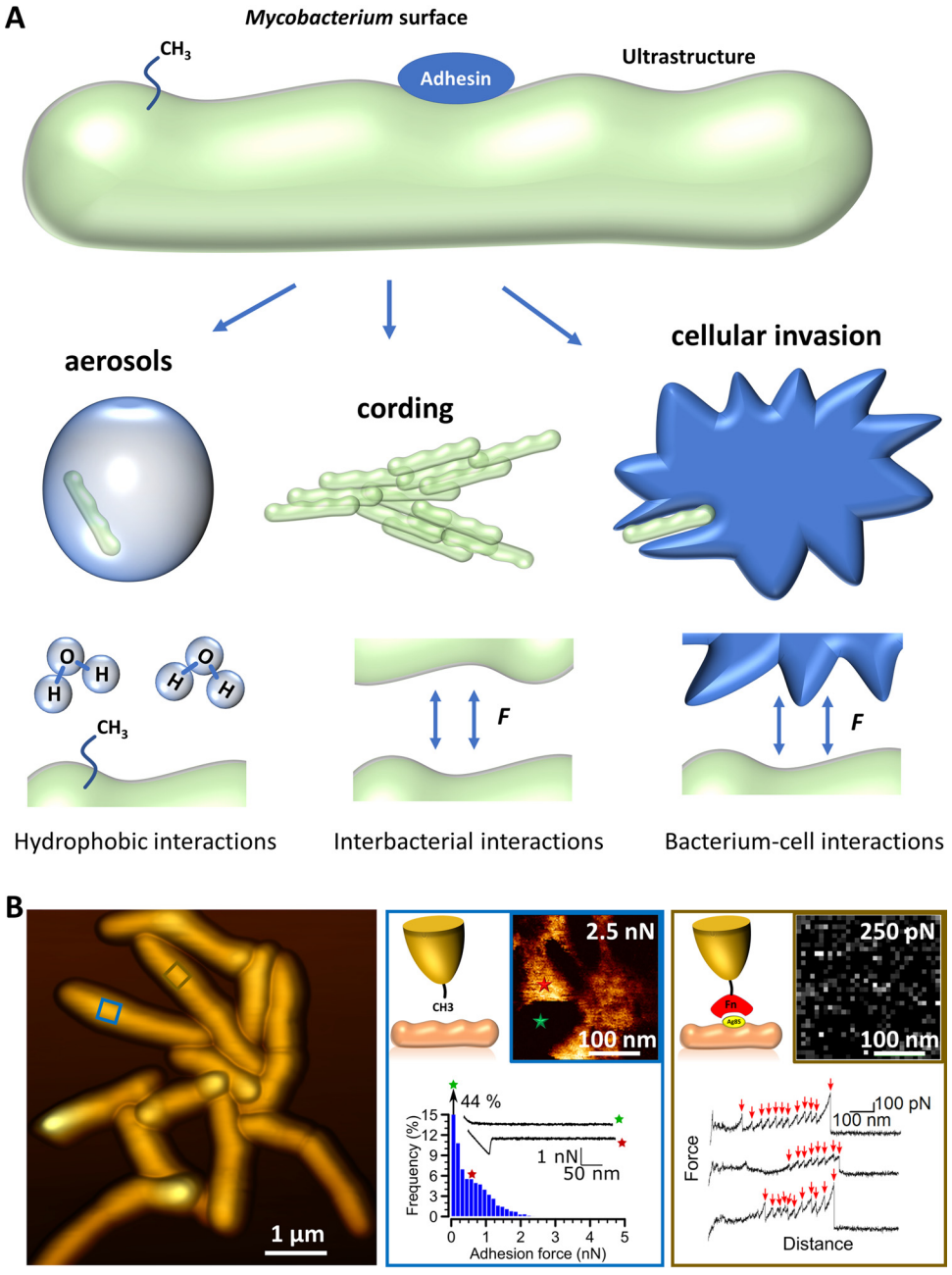

FIG 2 Interactions between mycobacterial surfaces and their environment. (A) Mycobacteria rely on hydrophobic properties of their surfaces to associate with aerosol droplets and to adhere to each other and form cords. Specialized adhesins stimulate mycobacterium-mycobacterium interactions as well as adhesion of mycobacteria to extracellular matrix proteins and cells. (B) Using AFM force spectroscopy to probe mycobacterial morphology, chemical properties, and adhesin interactions. (Left) A 3D projection of a height image showing a microcolony of *Mycobacterium abscessus* cells. (Center, top left) AFM probes exposing hydrophobic methyl groups have unraveled hydrophobic properties of mycobacterial cells. (Center, top right) Striking hydrophobic (lighter yellow, maximum of 2.5 nN) and hydrophilic (darker brown, minimum of 0 nN) nanodomains were seen on very high-resolution adhesion maps recorded on the surfaces of *M. abscessus* smooth variant (glycopeptidolipid$^+$) cells. (Center, bottom) Typical force-distance curves obtained as well as the histogram plot of the frequency distributions of hydrophobic adhesion forces. The red star is indicative of when hydrophobic adhesive forces were registered, whereas the green star indicates when no hydrophobic adhesive forces were registered. Adapted with permission from reference 61. (Right) AFM probe exposing single molecules of the host extracellular matrix protein, fibronectin (Fn), to which mycobacterial antigen 85 (Ag85, yellow oval) binds. The adhesion map in the top right corner shows a homogenous distribution of Ag85 on the surface of an *M. abscessus* cell. The white pixels represent single adhesins, with the lightest shade representing a maximum adhesion strength of 250 pN and the darkest pixels representing zero adhesion force. Typical force-distance curves of this specific receptor-ligand interaction are shown at the bottom. The sawtooth unbinding peaks highlighted by red arrows relate to sequential unfolding of repeat domains in Fn. Adapted from reference 48.

strengthening the HBHA-heparin interaction, suggesting that clustering of HBHA on the bacterial cell surface may drive strong adhesion. Indeed, AFM tips modified with heparin molecules could probe interactions with HBHA on living mycobacterial cells, allowing mapping of their nanoscale localization and revealing that the adhesins clustered within nanodomains on the bacterial surface. This phenomenon may favor the recruitment of proteoglycan receptors within lipid rafts (35). A similar approach using HBHA-modified tips revealed a homogenous distribution of HSPG receptors on living pneumocytes (36). Interestingly, when the AFM tip was retracted at high speeds (high pulling velocities), force curve signatures were observed that are typical for the extraction of plasma membrane tethers, structures that may play a role in host cell invasion. When it comes to homophilic interactions, SMFS unveiled a bimodal force distribution (~70 and 130 pN) for HBHA-HBHA interactions, indicating the participation of multimers in the coiled-coil-dependent interaction (37). AFM SMFS studies also demonstrated the involvement of both C-terminal and N-terminal domains of HBHA in its interaction with actin (36). Another question that AFM studies helped to address about HBHA regarded its surface localization despite the absence of a signal peptide directing its secretion via traditional protein secretion systems. SMFS with heparin-functionalized probes demonstrated a sharp decrease in detection of the HBHA-heparin force signature on *Mycobacterium smegmatis* cells lacking its orthologue of the putative preprotein translocase Rv0613c (38). Taken together, HBHA served as an excellent platform to explore how AFM SMFS studies could be applied to mycobacterial adhesins to reveal the forces whereby they interact with their ligands, to explore their interaction with different ligands, and to map the locations of adhesins on the mycobacterial surface at the nanoscale.

Mycobacteria also employ adhesins that specifically bind to extracellular matrix proteins, such as fibronectin (Fn) (39–41). The interaction between Fn and Fn-binding proteins (FnBPs) in *Mycobacterium bovis* BCG has also been investigated by SMFS (42, 43). Force mapping revealed a homogenous distribution of FnBPs on the surfaces of these mycobacteria, which was altered by treatment with polysaccharide-degrading enzymes or AG-targeting ethambutol, indicating that the major mycobacterial FnBPs are associated with the mycomembrane and not anchored to the plasma membrane. Although the major specific mycobacterial FnBP was not identified in this study, prime candidates are the Fn attachment protein (Fap) encoded by *Rv1860* that was originally identified in *Mycobacterium avium* (44) and the multifunctional antigen 85 (Ag85) complex (40). All members of the Ag85 complex possess a highly conserved and unique-to-mycobacteria Fn-binding sequence (40, 45, 46). In the multidrug-resistant, emerging, nontuberculous pathogen *Mycobacterium abscessus*, a single Fap orthologue shows poor conservation of the sequences necessary for Fn binding, while four Ag85 orthologues are present with highly conserved Fn-binding domains (45, 47). *M. abscessus* could thus be used to study the Ag85-Fn-specific interaction by SMFS (Fig. Fig. 2B, right panel) (48). Blocking experiments with peptides containing specific binding site sequences of either Fn or Ag85 demonstrated specificity of the interaction and that the Ag85 complex counts for the major Fn-binding activity in this mycobacterium. Notably, it was observed that the Ag85-Fn-specific interaction appeared to be mechanically activated with a sharp increase in binding forces from ~75 pN at low pulling speeds to ~500 pN at greater speeds. Moreover, modeling of the force-loading rate dependency using Friddle-Noy-de Yoreo theory (49) allowed calculation of thermodynamic parameters of the interaction, including the dissociation constant. The strong bonds observed under high tensile loading may favor strong mycobacterial attachment in the lung where cells are exposed to high shear stress or during hematogenous spread leading to a disseminated infection (28). Single-molecule experiments might soon reveal more stress-sensitive adhesins among mycobacteria. In the same line, molecular recognition experiments may be used to study the interactions between host cell receptors, such as lectins and their mycobacterial lipid ligands.

CELL ENVELOPE LIPIDS DEFINE HYDROPHOBIC AND HYDROPHILIC CELL-SURFACE NANODOMAINS

Hydrophobic forces are involved in many molecular processes, such as protein folding, membrane fusion, and cell adhesion. In pathogenesis, they often favor the adhesion of the bacteria to surfaces and tissues (50). In mycobacteria, the cell surface is rich in hydrophobic mycolic acids and their substantial surface hydrophobicity underlies their transmission via aerosols (3–5) and the ability of virulent strains to form cords (10). Therefore, assessing this property is an important issue (Fig. 2A). While the hydrophobic nature of the mycobacterial cell envelope is highly documented, the hydrophobicity of single mycobacterial cells and, in particular, the distribution of hydrophobic groups on their surfaces have been under explored. In this regard, AFM force spectroscopy with hydrophobic tips has proved to be a valuable method to measure local hydrophobic forces on living mycobacteria (51, 52). In the case of *M. bovis* BCG, a uniform and, unsurprisingly, very hydrophobic cell surface was observed that corresponded with force measurements made on model substrates coated with self-assembled monolayers of alkanethiols, exposing hydrophobic methyl groups (52, 53). Notably, treatment of cells with antitubercular drugs that inhibit the synthesis of mycolic acids (isoniazid) or AG (ethambutol) resulted in sharp decreases in hydrophobic adhesive forces measured on some cells. On other cells, hydrophilic nanodomains appeared, likely because of the loss of outer layers of the mycomembrane exposing a deeper (PG) hydrophilic layer (51, 53). These results indicate that the hydrophobic character of mycobacterial cells is conferred by mycolic acids exposed on their surfaces.

Several nontuberculous mycobacteria, including the pathogens *M. avium* and *M. abscessus*, produce large quantities of a class of surface-exposed polar lipids (less hydrophobic than mycolic acids) known as glycopeptidolipids (GPLs) (54). In *M. abscessus*, the irreversible transition from a GPL^+ to GPL^- phenotype directly correlates with a clinically important change from a smooth to a rough colony morphotype (54). The rough variant tends to grow as cords of bacteria tightly packed against each other, a physical arrangement that protects them from the host immune system and antimicrobials, making infections with this variant severe and very challenging to treat (55–57). Conversely, GPLs appear to be necessary for optimal biofilm formation and play immunomodulatory roles that may be important during early stages of infection (58–60). Recently, newly developed multiparametric AFM imaging with improved spatial resolution revealed striking hydrophobic and hydrophilic nanodomains that were only present on a GPL^+ *M. abscessus* strain (Fig. 2B, middle panel) (61). Hydrophilic nanodomains may thus represent areas in which more polar GPL classes are concentrated, while hydrophobic nanodomains mainly contain more apolar GPLs and/or mycolic acids. Such partitioning of surface lipids suggests a role for the spatial variation of hydrophobic properties in adhesion and biofilm formation. With GPLs masking proinflammatory lipid factors while being highly immunogenic themselves (62–64), nanodomains enriched in GPLs (or certain classes of GPLs) or in which GPLs are more sparse may also play a role in antigen presentation. Importantly, the compound BM212 that inhibits the essential mycolic acid flippase induced a sharp reduction in surface hydrophobicity of both smooth and rough variants (61), highlighting, along with the earlier work done on *M. bovis* BCG, the antiadhesive activity of antituberculars that target mycolic acid synthesis or transport (51, 53).

EFFECT OF ANTIBIOTICS ON THE MYCOMEMBRANE

The combination of AFM with antibiotic treatments represents a valuable approach to decipher the very complex architecture of the mycobacterial cell wall and may help us understand how structural alterations of the wall lead to cell death. Initial investigations of mycobacterial surfaces revealed smooth surfaces (52, 65). However, treatment with both cell-wall active drugs (isoniazid, ethionamide, and ethambutol) and an antibiotic targeting protein translation (streptomycin) led to alterations on *M. bovis* BCG surfaces, increasing their roughness (51). In the case of ethambutol that targets AG

specifically, concentric striations were observed at its MIC, while at concentrations above the MIC, an additional perpendicular layer also exhibiting concentric striations became apparent (65). These different layers may be partially synthesized and, hence, nonesterified AG and underlying PG, respectively. This view is supported by the fact that surface alterations were accompanied by a dramatic loss of surface hydrophobicity, probably due to the loss of the mycolic-acid rich mycomembrane (51). The functional consequences of AG inhibition by ethambutol and isoniazid on cell wall nanomechanics were investigated in real time (66). Both antitubercular drugs led to sharp decreases in cell wall stiffness and elasticity, which showed different time dependencies. Interestingly, the nanomechanical effect of ethambutol was cell cycle dependent (67), with cells at different division phases showing different responses to the drug. More recently, it was found that in the absence of the L,D-transpeptidase activity responsible for the noncanonical 3-3 cross-links that are abundant in mycobacterial PG, the bacteria exhibited alterations in cell wall stiffness and were more sensitive to drugs inhibiting the enzymes responsible for canonical 4-3 cross-links (68).

Focusing on deeper layers of the mycobacterial cell envelope, immunogold AFM imaging of ethambutol- or isoniazid-treated *M. bovis* BCG detected and localized lipoarabinomannan (LAM) on the surfaces of these cells but not on the surfaces of untreated cells (51). SMFS studies utilizing anti-LAM antibody-functionalized AFM tips later confirmed these results (69). Molecular mapping of LAM on untreated *M. bovis* BCG cells showed that LAM was present at very low levels on these cell surfaces ($<$5% binding frequency). On isoniazid-treated cells, anti-LAM-LAM interactions occurred at a high frequency, and force maps revealed that LAM clustered into nanodomains in these cells, probably reflecting areas in which the mycomembrane had been disrupted.

Considering differences in the lipid compositions and antibiotic susceptibilities between different mycobacterial species, in particular between tubercle bacilli and nontuberculous mycobacteria, future AFM studies are warranted to delineate the ultrastructural changes that occur on the bacterial cell surfaces under exposure to different classes of antibiotics.

CELL GROWTH DYNAMICS

Cell growth and subsequent cell division are two essential phases of proliferation for all bacterial species. The macromolecular mechanisms underlying growth and division in mycobacteria are different from other bacterial genera (70). Bacterial cell growth is accomplished by localized PG synthesis at distinct regions, such as the septum (*Staphylococcus aureus*), the lateral cell wall (*Bacillus subtilis*, *Escherichia coli*), or the poles (*Mycobacterium* species) (12, 71). Studying the polar growth at subdiffractional level revealed that the site of growth is guided by the tropomyosin-like protein DivIVA/Wag31, which is located at the cell tip, whereas the enzymes for cell wall biogenesis are located subpolarly (72). Mycobacterial cell elongation and division lead to daughter cells of different sizes (14, 73–75), which gives rise to population heterogeneity. This heterogeneity may be beneficial for the survival in the host and under antibiotic pressure (14, 70, 76). There has been controversy about the pattern of mycobacterial single-cell growth. While a unipolar growth model proposes that cells elongate preferentially at the old pole (OP) between cell birth and division (14), a bipolar model suggests that both poles elongate at equal rates during the period between cell separation and cytokinesis with a subsequent predominant growth of the OP (74). Recently, it was shown that mycobacterial cell growth neither follows a unipolar nor a bipolar pattern. Instead, a biphasic growth model for the new pole (NP) was proposed based on time-lapse correlative AFM-optical microscopy (Fig. 3A) imaging of *Mycobacterium smegmatis*. This model was confirmed for other pathogenic species (*Mycobacterium tuberculosis*, *Mycobacterium abscessus*, *Mycobacterium marinum*) using optical microscopy (77). A rate-change transition was observed at the newly born pole from a slow-growing to a fast-growing state with a delay of variable time length ("new end take off"

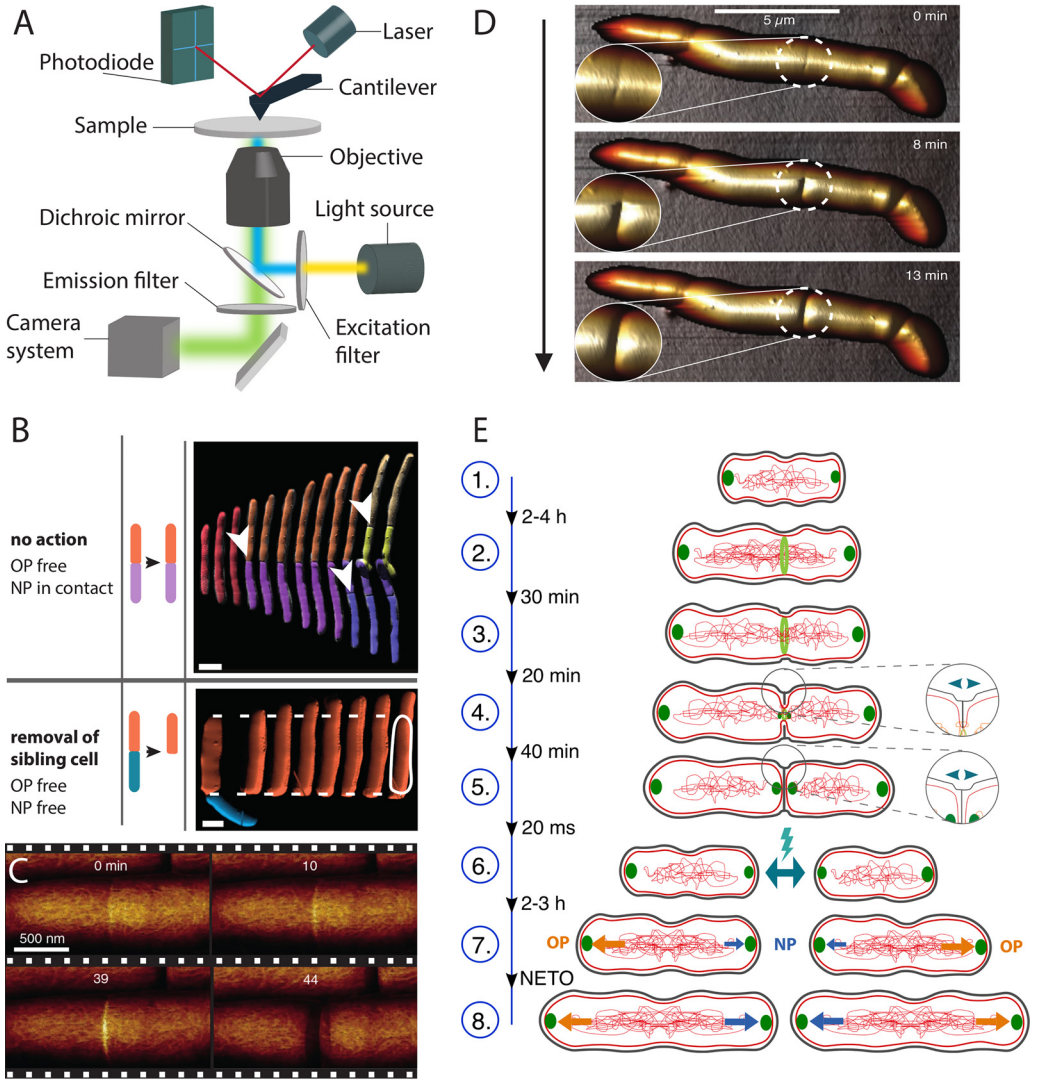

FIG 3 Studying cell growth dynamics with a correlative AFM-optical microscope. (A) Schematic representation of a correlative AFM-optical microscope. The field of view of an inverted fluorescence microscope is aligned with the cantilever of an AFM in order to acquire correlated images. (B) AFM used as a nanomanipulation tool. Schematics and time-lapse AFM of growing mycobacteria. (Top) Sibling cells are kept in their original position after cell division. Poles of mother and daughter cells are in close contact. (Bottom) The AFM cantilever was used to remove one of the sibling cells to avoid physical constraints on the new pole (NP, OP being the old pole). Arrowheads point to the division site. Adapted from reference 77. (C) AFM stiffness measurement of cell surface at the division site between the emergence of the precleavage furrow (PCF) and cleavage. Lighter colors represent a higher stiffness. (D). Three-dimensional rendered AFM topographic images of *Mycobacterium smegmatis* before cell cleavage and enlargements of the area around precleavage furrow. The arrow indicates increasing time. The top panel was scanned from bottom to top, the middle panel was scanned from top to bottom and the bottom panel was scanned from bottom to top. (C, D) Adapted from reference 86 with permission. (E) Schematic representation of the consecutive events leading to cell division in *Mycobacterium smegmatis* studied by correlative AFM-optical microscopy. (1) At cell birth (division of the mother cell), Wag31-green fluorescent protein (GFP) (dark green) is localized only at the poles. The cell surface comprises wavelike morphological features, and the subsequent cell division occurs at the centermost trough near midcell. (2) FtsZ-GFP (light green) localizes at the central wave trough and forms a circumferential ring. (3) Formation of the precleavage furrow starts, which is colocalized with the FtsZ ring. (4) Stress builds up, whereas membrane strength decreases at precleavage furrow. Septum formation and cytokinesis occur. Wag31-GFP localizes to the future division side, whereas the FtsZ ring disassembles. (5) The tensile stress increases. (6) Further increase of turgor pressure cumulates in physical cell separation by rapid mechanical rupture leading to newborn sibling cells. (The space between the sibling cells after division was inserted for visualization purposes. In reality, the sibling cells stay in proximity to each other.) (7) Pre-NETO phase: low growth rate of the NP. Reallocation of Wag31 from the OP to the NP. (8) Post-NETO phase: growth rate change (NETO) is followed by a high growth rate of the NPs. The OPs grow in both phases with a constant, high rate.

[NETO]), whereas the OP showed a fast and constant growth. This rate-change occurred mostly before cell division but also occurred occasionally after cell division. NETO and the event of cell division are therefore not linked. Instead, the degree of growth asymmetry at cell division depends on the difference between NETO delay and interdivision time. By using the AFM tip as a nanomanipulator to lyse or remove the neighboring sibling cell, they showed that the pre-NETO time is not caused by physical constraints (Fig. 3B). In order to investigate whether the delay before NETO is associated with a delayed relocalization of the molecules required for cell wall biogenesis, the authors studied the localization of DivIVA/Wag31. They observed a partial relocalization of DivIVA/Wag31 from the old to the new poles during the pre-NETO phase (77).

Bacterial growth is followed by cell division, which is a spatially and temporally highly coordinated process (78). This process involves the selection of the time point and location of the division site (79), control of synthesis, and disassembly of cell wall components at the division site, while maintaining integrity (80) and cell shape (12). Because mycobacteria have a complex cell wall, the mechanisms underlying cell division differ from other bacterial models (78). Using high-resolution microscopy techniques, morphological features of the cell surface were identified and linked to the inception and completion of bacterial division. Investigations with electron microscopy (scanning electron microscopy and transmission electron microscopy) revealed circular division scars at the newly formed poles after cell separation (81, 82). As AFM enables live-cell studies, morphological characteristics during the cell separation process, including the emergence of a septal furrow prior to division, could be observed in real time (Fig. 3C and D) (67). The ability of AFM to measure three-dimensional (3D) profiles revealed waveform troughs on the corrugated cell surface of *Mycobacterium smegmatis* (11). Employing time-lapse single-cell imaging, the centermost trough near midcell was linked to the division site, which points to the importance of wave troughs as the earliest known reference point for the future division site. Long-term imaging over several generations showed that cells inherit these morphological features from the (grand)mother cell. Assembly of the FtsZ ring is localized at a preexisting wave trough near midcell position, as shown by correlative AFM-optical microscopy.

Mycobacterial cell division is coordinated by the divisome, a macromolecular complex of multiple proteins, including peptidoglycan synthases and hydrolases, which assembles at the midcell position to synthesize the septum before separation into two daughter cells (79, 83). Recent studies suggest that in addition to molecular mechanisms, mechanical forces are involved during the cell division process in *Staphylococcus aureus* and actinobacteria (84, 85). By deploying the capability of AFM to measure mechanical properties, the cooperation of localized enzymatic activity and mechanical forces to separate sibling cells was identified in *Mycobacterium smegmatis* (86). Turgor pressure, through a concentration of tensile stress at the precleavage furrow in combination with diminished material strength due to the enzymatic activity of RipA peptidoglycan hydrolase, leads to fast cell cleavage (Fig. 3C and D). In contrast, reducing cell wall hydrolysis by inducing decreased expression of RipA inhibits cell cleavage, which results in chains of nongrowing cells where only the two outermost poles elongate. By using AFM as a nanomanipulation tool to apply additional force on the septum, direct cell cleavage was observed even for chained RipA-depleted cells. Taken together, these AFM investigations provide a detailed picture of the mycobacterial cell division in time and space (Fig. 3E). After birth, the cell elongates by creating new wave troughs (Fig. 3E, 1). Approximately 2 to 4 h after cell birth, the FtsZ ring starts to form in the centermost wave trough (Fig. 3E, 2). Shortly after, a small circumferential band occurs colocated with the FtsZ ring (Fig. 3E, 3). This precleavage furrow is only a few nanometers deep. The stiffness of the precleavage furrow steadily increases as cell division progresses. Once cytokinesis is complete, Wag31 appears to be colocated with the precleavage furrow (Fig. 3E, 4). The localized stress in the membrane continues to increase (Fig. 3E, 5). Once the stress at the

precleavage furrow exceeds the tensile strength of the cell wall material, the bacteria separate abruptly in what appears to be a turgor pressure-driven fracture process (Fig. 3E, 6). After cell separation, the OPs continue to grow at their previous growth velocity; however, the NPs initially grow significantly slower (Fig. 3E,7). After a while, the NP undergoes a transition in growth velocity from the slow regime to the same growth velocity as the OP (NETO) (Fig. 3E, 8). At this point, the cycle begins again.

CONCLUSIONS

AFM studies have brought important new insights into mycobacterial structure, function, and physiology. Nanoscale mapping of the surface of living mycobacteria with specific functionalized AFM probes has enabled determination of the strength and dynamics of adhesin-ligand interactions and quantification of chemical properties like surface hydrophobicity. Time-lapse imaging has contributed to our understanding of mycobacterial division and growth, surface ultrastructure, and how the latter is altered by cell wall active antibiotics. What lies ahead?

Beyond the examples reviewed herein, huge untapped potential exists for the use of AFM technologies in the study of mycobacteria. Real-time correlative and multiparametric imaging has already proven its merit to correlate cellular processes with ultrastructural, chemical, and mechanical characteristics of the mycomembrane. While important discoveries were made relating to growth and division of model mycobacteria under optimal growth conditions, the next steps would include addressing the nanoscale surface characteristics of clinically important mycobacteria, including *Mycobacterium tuberculosis*, under conditions that are more relevant to their pathogenesis.

Force spectroscopy modes have been helpful to characterize the interactions between mycobacterial adhesins and host factors, but the potential to combine SMFS molecular recognition with topographic imaging, an approach that has delivered numerous insights into surface protein clustering (87), has not been delved into for mycobacteria. Several mycobacterial proteins and lipids were identified that act as adhesins binding to host factors, but these interactions remain poorly characterized (7, 8). In addition to unravelling the molecular forces in the interactions between cognate ligands and mycobacterial adhesins (or surface components recognized by immune cell receptors), SMFS may serve as a platform to characterize thermodynamic and kinetic parameters of these interactions and may present an excellent tool to discover compounds with therapeutic potential. Also, the potential of SCFS studies to investigate direct cell-cell interactions, for example between individual mycobacterial cells or between single bacteria and single host cells, has not been explored. This approach has been applied with massive payoff in the investigation of cell adhesion of a number of Gram-positive and -negative pathogens (88).

Some exciting AFM technologies still need to see their first use in the study of mycobacteria. High-speed AFM (HS-AFM) has been used to make movies of integral membrane proteins, such as transporters performing their activities in real time (18, 19, 89). HS-AFM may offer a solution for the analysis of substrate transport dynamics in mycobacterial antibiotic efflux pumps and mycomembrane lipid transporters, for which bioassays are scarce. Another exciting AFM technology that has yet to be used with mycobacteria is fluidic force microscopy (FluidFM) (90–92), where microchanneled cantilevers with micro- or nanosized apertures allow for fast manipulation of single cells. This recent technology may thus prove to be incredibly useful to rapidly assay the forces with which different mycobacterial strains or mutants (e.g., lacking surface-exposed lipids) bind host macrophage cells in the step preceding cellular invasion.

Many questions remain regarding the complex ultrastructure of the mycobacterial envelope, which seems to vary significantly between single cells, particularly during different stages of infection (2). There are also unsolved questions regarding the unique asymmetric growth dynamics of mycobacteria, resulting in sister cells having distinct characteristics (13, 70). As AFM technology is continuously evolving with

higher speed, greater force sensitivity and stability, and higher resolution (18), we are confident that many of these problems will be resolved in the next decade.

ACKNOWLEDGMENTS

Work at UCLouvain was supported by the Excellence of Science-EOS program (grant no. 30550343), the European Research Council (ERC) under the European Union's Horizon 2020 research and innovation program (grant agreement no. 693630), the FNRS-WELBIO (grant no. WELBIO-CR-2015A-05), the National Fund for Scientific Research (FNRS), and the Research Department of the Communauté française de Belgique (Concerted Research Action). Work at EPFL was supported by the ERC through CoG-773091: InCell to G.E.F., and the Swiss National Science Foundation through grant 200021_182562 to G.E.F. and through grants 310030B_176397 and IZLSZ3_170912 to J.D.M. Y.F.D. is research director at the FNRS.

The funders had no role in study design, data collection and analysis, decision to publish, or preparation of the manuscript.

A.V., E.R., J.D.M., G.E.F., and Y.F.D. wrote the manuscript. J.D.M., G.E.F., and Y.F.D. supervised the work.

We declare that no competing interests exist.

REFERENCES

1. Jarlier V, Nikaido H. 1994. Mycobacterial cell wall: structure and role in natural resistance to antibiotics. FEMS Microbiol Lett 123:11–18. https://doi.org/10.1111/j.1574-6968.1994.tb07194.x.
2. Dulberger CL, Rubin EJ, Boutte CC. 2020. The mycobacterial cell envelope—a moving target. Nat Rev Microbiol 18:47–59. https://doi.org/10.1038/s41579-019-0273-7.
3. Falkinham JO. 2003. Mycobacterial aerosols and respiratory disease. Emerg Infect Dis 9:763–767. https://doi.org/10.3201/eid0907.020415.
4. Cambier CJ, Falkow S, Ramakrishnan L. 2014. Host evasion and exploitation schemes of *Mycobacterium tuberculosis*. Cell 159:1497–1509. https://doi.org/10.1016/j.cell.2014.11.024.
5. Jankute M, Nataraj V, Lee OY-C, Wu HHT, Ridell M, Garton NJ, Barer MR, Minnikin DE, Bhatt A, Besra GS. 2017. The role of hydrophobicity in tuberculosis evolution and pathogenicity. Sci Rep 7:1315. https://doi.org/10.1038/s41598-017-01501-0.
6. Pethe K, Alonso S, Biet F, Delogu G, Brennan MJ, Locht C, Menozzi FD. 2001. The heparin-binding haemagglutinin of *M. tuberculosis* is required for extrapulmonary dissemination. Nature 412:190–194. https://doi.org/10.1038/35084083.
7. Govender VS, Ramsugit S, Pillay M. 2014. *Mycobacterium tuberculosis* adhesins: potential biomarkers as anti-tuberculosis therapeutic and diagnostic targets. Microbiology (Reading) 160:1821–1831. https://doi.org/10.1099/mic.0.082206-0.
8. Vinod V, Vijayrajratnam S, Vasudevan AK, Biswas R. 2020. The cell surface adhesins of *Mycobacterium tuberculosis*. Microbiol Res 232:126392. https://doi.org/10.1016/j.micres.2019.126392.
9. Middlebrook G, Dubos RJ, Pierce C. 1947. Virulence and morphological characteristics of mammalian tubercle bacilli. J Exp Med 86:175–184. https://doi.org/10.1084/jem.86.2.175.
10. Bloch H, Sorkin E, Erlenmeyer H. 1953. A toxic lipid component of the tubercle bacillus (cord factor). I. Isolation from petroleum ether extracts of young bacterial cultures. Am Rev Tuberc 67:629–643. https://doi.org/10.1164/art.1953.67.5.629.
11. Eskandarian HA, Odermatt PD, Ven JXY, Hannebelle MTM, Nievergelt AP, Dhar N, McKinney JD, Fantner GE. 2017. Division site selection linked to inherited cell surface wave troughs in mycobacteria. Nat Microbiol 2:17094. https://doi.org/10.1038/nmicrobiol.2017.94.
12. Cabeen MT, Jacobs-Wagner C. 2005. Bacterial cell shape. Nat Rev Microbiol 3:601–610. https://doi.org/10.1038/nrmicro1205.
13. Baranowski C, Rego EH, Rubin EJ. 2019. The dream of a mycobacterium. Microbiol Spectr 7:GPP3-0008-2018. https://doi.org/10.1128/microbiolspec.GPP3-0008-2018.
14. Aldridge BB, Fernandez-Suarez M, Heller D, Ambravaneswaran V, Irimia D, Toner M, Fortune SM. 2012. Asymmetry and aging of mycobacterial cells lead to variable growth and antibiotic susceptibility. Science 335:100–104. https://doi.org/10.1126/science.1216166.
15. Dhar N, McKinney J, Manina G. 2016. Phenotypic heterogeneity in *Mycobacterium tuberculosis*. Microbiol Spectr 4:TBTB2-0021-2016. https://doi.org/10.1128/microbiolspec.TBTB2-0021-2016.
16. Dufrêne YF. 2008. Towards nanomicrobiology using atomic force microscopy. Nat Rev Microbiol 6:674–680. https://doi.org/10.1038/nrmicro1948.
17. Dufrêne YF, Ando T, Garcia R, Alsteens D, Martinez-Martin D, Engel A, Gerber C, Müller DJ. 2017. Imaging modes of atomic force microscopy for application in molecular and cell biology. Nat Nanotechnol 12:295–307. https://doi.org/10.1038/nnano.2017.45.
18. Ando T. 2018. High-speed atomic force microscopy and its future prospects. Biophys Rev 10:285–292. https://doi.org/10.1007/s12551-017-0356-5.
19. Heath GR, Scheuring S. 2019. Advances in high-speed atomic force microscopy (HS-AFM) reveal dynamics of transmembrane channels and transporters. Curr Opin Struct Biol 57:93–102. https://doi.org/10.1016/j.sbi.2019.02.008.
20. Dufrêne YF, Pelling AE. 2013. Force nanoscopy of cell mechanics and cell adhesion. Nanoscale 5:4094–4104. https://doi.org/10.1039/c3nr00340j.
21. Dufrêne YF, Martínez-Martín D, Medalsy I, Alsteens D, Müller DJ. 2013. Multiparametric imaging of biological systems by force-distance curve-based AFM. Nat Methods 10:847–854. https://doi.org/10.1038/nmeth.2602.
22. Alsteens D, Müller DJ, Dufrêne YF. 2017. Multiparametric atomic force microscopy imaging of biomolecular and cellular systems. Acc Chem Res 50:924–931. https://doi.org/10.1021/acs.accounts.6b00638.
23. Bermudez LE, Goodman J. 1996. *Mycobacterium tuberculosis* invades and replicates within type II alveolar cells. Infect Immun 64:1400–1406. https://doi.org/10.1128/IAI.64.4.1400-1406.1996.
24. Ashiru OT, Pillay M, Sturm AW. 2010. Adhesion to and invasion of pulmonary epithelial cells by the F15/LAM4/KZN and Beijing strains of *Mycobacterium tuberculosis*. J Med Microbiol 59:528–533. https://doi.org/10.1099/jmm.0.016006-0.
25. Ashiru OT, Pillay M, Sturm AW. 2012. *Mycobacterium tuberculosis* isolates grown under oxygen deprivation invade pulmonary epithelial cells. Anaerobe 18:471–474. https://doi.org/10.1016/j.anaerobe.2012.04.010.
26. Bhattacharya J, Westphalen K. 2016. Macrophage-epithelial interactions in pulmonary alveoli. Semin Immunopathol 38:461–469. https://doi.org/10.1007/s00281-016-0569-x.
27. Russell DG. 2007. Who puts the tubercle in tuberculosis? Nat Rev Microbiol 5:39–47. https://doi.org/10.1038/nrmicro1538.
28. Clark RA, Blakley SL, Greer D, Smith MH, Brandon W, Wisniewski TL. 1991. Hematogenous dissemination of *Mycobacterium tuberculosis* in patients with AIDS. Rev Infect Dis 13:1089–1092. https://doi.org/10.1093/clinids/13.6.1089.
29. Stokes RW, Norris-Jones R, Brooks DE, Beveridge TJ, Doxsee D, Thorson LM. 2004. The glycan-rich outer layer of the cell wall of *Mycobacterium tuberculosis* acts as an antiphagocytic capsule limiting the association of

the bacterium with macrophages. Infect Immun 72:5676–5686. https://doi.org/10.1128/IAI.72.10.5676-5686.2004.
30. Hinterdorfer P, Dufrêne YF. 2006. Detection and localization of single molecular recognition events using atomic force microscopy. Nat Methods 3:347–355. https://doi.org/10.1038/nmeth871.
31. Delogu G, Brennan MJ. 1999. Functional domains present in the mycobacterial hemagglutinin, HBHA. J Bacteriol 181:7464–7469. https://doi.org/10.1128/JB.181.24.7464-7469.1999.
32. Pethe K, Aumercier M, Fort E, Gatot C, Locht C, Menozzi FD. 2000. Characterization of the heparin-binding site of the mycobacterial heparin-binding hemagglutinin adhesin. J Biol Chem 275:14273–14280. https://doi.org/10.1074/jbc.275.19.14273.
33. Menozzi FD, Reddy VM, Cayet D, Raze D, Debrie A-S, Dehouck M-P, Cecchelli R, Locht C. 2006. *Mycobacterium tuberculosis* heparin-binding haemagglutinin adhesin (HBHA) triggers receptor-mediated transcytosis without altering the integrity of tight junctions. Microbes Infect 8:1–9. https://doi.org/10.1016/j.micinf.2005.03.023.
34. Dupres V, Menozzi FD, Locht C, Clare BH, Abbott NL, Cuenot S, Bompard C, Raze D, Dufrêne YF. 2005. Nanoscale mapping and functional analysis of individual adhesins on living bacteria. Nat Methods 2:515–520. https://doi.org/10.1038/nmeth769.
35. Tkachenko E, Simons M. 2002. Clustering induces redistribution of syndecan-4 core protein into raft membrane domains. J Biol Chem 277:19946–19951. https://doi.org/10.1074/jbc.M200841200.
36. Verbelen C, Dupres V, Raze D, Bompard C, Locht C, Dufrêne YF. 2008. Interaction of the mycobacterial heparin-binding hemagglutinin with actin, as evidenced by single-molecule force spectroscopy. J Bacteriol 190:7614–7620. https://doi.org/10.1128/JB.00974-08.
37. Verbelen C, Raze D, Dewitte F, Locht C, Dufrêne YF. 2007. Single-molecule force spectroscopy of mycobacterial adhesin-adhesin interactions. J Bacteriol 189:8801–8806. https://doi.org/10.1128/JB.01299-07.
38. Veyron-Churlet R, Dupres V, Saliou J-M, Lafont F, Raze D, Locht C. 2018. Rv0613c/MSMEG_1285 interacts with HBHA and mediates its proper cell-surface exposure in mycobacteria. Int J Mol Sci 19:1673. https://doi.org/10.3390/ijms19061673.
39. Ratliff TL, McGarr JA, Abou-Zeid C, Rook GA, Stanford JL, Aslanzadeh J, Brown EJ. 1988. Attachment of mycobacteria to fibronectin-coated surfaces. J Gen Microbiol 134:1307–1313. https://doi.org/10.1099/00221287-134-5-1307.
40. Abou-Zeid C, Ratliff TL, Wiker HG, Harboe M, Bennedsen J, Rook GA. 1988. Characterization of fibronectin-binding antigens released by *Mycobacterium tuberculosis* and *Mycobacterium bovis* BCG. Infect Immun 56:3046–3051. https://doi.org/10.1128/IAI.56.12.3046-3051.1988.
41. Abou-Zeid C, Garbe T, Lathigra R, Wiker HG, Harboe M, Rook GA, Young DB. 1991. Genetic and immunological analysis of *Mycobacterium tuberculosis* fibronectin-binding proteins. Infect Immun 59:2712–2718. https://doi.org/10.1128/IAI.59.8.2712-2718.1991.
42. Verbelen C, Dufrêne YF. 2009. Direct measurement of *Mycobacterium*-fibronectin interactions. Integr Biol (Camb) 1:296–300. https://doi.org/10.1039/b901396b.
43. Hall-Stoodley L, Watts G, Crowther JE, Balagopal A, Torrelles JB, Robison-Cox J, Bargatze RF, Harmsen AG, Crouch EC, Schlesinger LS. 2006. *Mycobacterium tuberculosis* binding to human surfactant proteins A and D, fibronectin, and small airway epithelial cells under shear conditions. Infect Immun 74:3587–3596. https://doi.org/10.1128/IAI.01644-05.
44. Schorey JS, Li Q, McCourt DW, Bong-Mastek M, Clark-Curtiss JE, Ratliff TL, Brown EJ. 1995. A *Mycobacterium leprae* gene encoding a fibronectin binding protein is used for efficient invasion of epithelial cells and Schwann cells. Infect Immun 63:2652–2657. https://doi.org/10.1128/IAI.63.7.2652-2657.1995.
45. Naito M, Ohara N, Matsumoto S, Yamada T. 1998. The novel fibronectin-binding motif and key residues of mycobacteria. J Biol Chem 273:2905–2909. https://doi.org/10.1074/jbc.273.5.2905.
46. Kuo C-J, Bell H, Hsieh C-L, Ptak CP, Chang Y-F. 2012. Novel mycobacteria antigen 85 complex binding motif on fibronectin. J Biol Chem 287:1892–1902. https://doi.org/10.1074/jbc.M111.298687.
47. Schorey JS, Holsti MA, Ratliff TL, Allen PM, Brown EJ. 1996. Characterization of the fibronectin-attachment protein of *Mycobacterium avium* reveals a fibronectin-binding motif conserved among mycobacteria. Mol Microbiol 21:321–329. https://doi.org/10.1046/j.1365-2958.1996.6381353.x.
48. Viljoen A, Alsteens D, Dufrêne Y. 2020. Mechanical forces between mycobacterial antigen 85 complex and fibronectin. Cells 9:716. https://doi.org/10.3390/cells9030716.
49. Friddle RW, Noy A, Yoreo JJD. 2012. Interpreting the widespread nonlinear force spectra of intermolecular bonds. Proc Natl Acad Sci U S A 109:13573–13578. https://doi.org/10.1073/pnas.1202946109.
50. Doyle RJ. 2000. Contribution of the hydrophobic effect to microbial infection. Microbes Infect 2:391–400. https://doi.org/10.1016/s1286-4579(00)00328-2.
51. Alsteens D, Verbelen C, Dague E, Raze D, Baulard AR, Dufrêne YF. 2008. Organization of the mycobacterial cell wall: a nanoscale view. Pflugers Arch 456:117–125. https://doi.org/10.1007/s00424-007-0386-0.
52. Dague E, Alsteens D, Latgé J-P, Verbelen C, Raze D, Baulard AR, Dufrêne YF. 2007. Chemical force microscopy of single live cells. Nano Lett 7:3026–3030. https://doi.org/10.1021/nl071476k.
53. Alsteens D, Dague E, Rouxhet PG, Baulard AR, Dufrêne YF. 2007. Direct measurement of hydrophobic forces on cell surfaces using AFM. Langmuir 23:11977–11979. https://doi.org/10.1021/la702765c.
54. Gutiérrez AV, Viljoen A, Ghigo E, Herrmann J-L, Kremer L. 2018. Glycopeptidolipids, a double-edged sword of the *Mycobacterium abscessus* complex. Front Microbiol 9:1145. https://doi.org/10.3389/fmicb.2018.01145.
55. Catherinot E, Roux A-L, Macheras E, Hubert D, Matmar M, Dannhoffer L, Chinet T, Morand P, Poyart C, Heym B, Rottman M, Gaillard J-L, Herrmann J-L. 2009. Acute respiratory failure involving an R variant of *Mycobacterium abscessus*. J Clin Microbiol 47:271–274. https://doi.org/10.1128/JCM.01478-08.
56. Nessar R, Cambau E, Reyrat JM, Murray A, Gicquel B. 2012. *Mycobacterium abscessus*: a new antibiotic nightmare. J Antimicrob Chemother 67:810–818. https://doi.org/10.1093/jac/dkr578.
57. Bernut A, Herrmann J-L, Kissa K, Dubremetz J-F, Gaillard J-L, Lutfalla G, Kremer L. 2014. *Mycobacterium abscessus* cording prevents phagocytosis and promotes abscess formation. Proc Natl Acad Sci U S A 111:E943–E952. https://doi.org/10.1073/pnas.1321390111.
58. Howard ST, Rhoades E, Recht J, Pang X, Alsup A, Kolter R, Lyons CR, Byrd TF. 2006. Spontaneous reversion of *Mycobacterium abscessus* from a smooth to a rough morphotype is associated with reduced expression of glycopeptidolipid and reacquisition of an invasive phenotype. Microbiology (Reading) 152:1581–1590. https://doi.org/10.1099/mic.0.28625-0.
59. Roux A-L, Viljoen A, Bah A, Simeone R, Bernut A, Laencina L, Deramaudt T, Rottman M, Gaillard J-L, Majlessi L, Brosch R, Girard-Misguich F, Vergne I, de Chastellier C, Kremer L, Herrmann J-L. 2016. The distinct fate of smooth and rough *Mycobacterium abscessus* variants inside macrophages. Open Biol 6:16018. https://doi.org/10.1098/rsob.160185.
60. Whang J, Back YW, Lee K-I, Fujiwara N, Paik S, Choi CH, Park J-K, Kim H-J. 2017. *Mycobacterium abscessus* glycopeptidolipids inhibit macrophage apoptosis and bacterial spreading by targeting mitochondrial cyclophilin D. Cell Death Dis 8:e3012. https://doi.org/10.1038/cddis.2017.420.
61. Viljoen A, Viela F, Kremer L, Dufrêne YF. 2020. Fast chemical force microscopy demonstrates that glycopeptidolipids define nanodomains of varying hydrophobicity on mycobacteria. Nanoscale Horiz 5:944–953. https://doi.org/10.1039/c9nh00736a.
62. Schorey JS, Sweet L. 2008. The mycobacterial glycopeptidolipids: structure, function, and their role in pathogenesis. Glycobiology 18:832–841. https://doi.org/10.1093/glycob/cwn076.
63. Rhoades ER, Archambault AS, Greendyke R, Hsu F-F, Streeter C, Byrd TF. 2009. *Mycobacterium abscessus* glycopeptidolipids mask underlying cell wall phosphatidyl-myo-inositol mannosides blocking induction of human macrophage TNF-α by preventing interaction with TLR2. J Immunol 183:1997–2007. https://doi.org/10.4049/jimmunol.0802181.
64. Davidson LB, Nessar R, Kempaiah P, Perkins DJ, Byrd TF. 2011. *Mycobacterium abscessus* glycopeptidolipid prevents respiratory epithelial TLR2 signaling as measured by HβD2 gene expression and IL-8 release. PLoS One 6:e29148. https://doi.org/10.1371/journal.pone.0029148.
65. Verbelen C, Dupres V, Menozzi FD, Raze D, Baulard AR, Hols P, Dufrêne YF. 2006. Ethambutol-induced alterations in *Mycobacterium bovis* BCG imaged by atomic force microscopy. FEMS Microbiol Lett 264:192–197. https://doi.org/10.1111/j.1574-6968.2006.00443.x.
66. Wu Y, Zhou A. 2009. *In situ*, real-time tracking of cell wall topography and nanomechanics of antimycobacterial drugs treated *Mycobacterium JLS* using atomic force microscopy. Chem Commun (Camb) 2009:7021–7023. https://doi.org/10.1039/b914605a.
67. Wu Y, Sims RC, Zhou A. 2014. AFM resolves effects of ethambutol on nanomechanics and nanostructures of single dividing mycobacteria in real-time. Phys Chem Chem Phys 16:19156–19164. https://doi.org/10.1039/c4cp01317d.
68. Baranowski C, Welsh MA, Sham L-T, Eskandarian HA, Lim HC, Kieser KJ, Wagner JC, McKinney JD, Fantner GE, Ioerger TR, Walker S, Bernhardt TG,

Rubin EJ, Rego EH. 2018. Maturing *Mycobacterium smegmatis* peptidoglycan requires non-canonical crosslinks to maintain shape. Elife 7:e37516. https://doi.org/10.7554/eLife.37516.
69. Verbelen C, Christiaens N, Alsteens D, Dupres V, Baulard AR, Dufrêne YF. 2009. Molecular mapping of lipoarabinomannans on mycobacteria. Langmuir 25:4324–4327. https://doi.org/10.1021/la900302a.
70. Kieser KJ, Rubin EJ. 2014. How sisters grow apart: mycobacterial growth and division. Nat Rev Microbiol 12:550–562. https://doi.org/10.1038/nrmicro3299.
71. Thanky NR, Young DB, Robertson BD. 2007. Unusual features of the cell cycle in mycobacteria: polar-restricted growth and the snapping-model of cell division. Tuberculosis (Edinb) 87:231–236. https://doi.org/10.1016/j.tube.2006.10.004.
72. Meniche X, Otten R, Siegrist MS, Baer CE, Murphy KC, Bertozzi CR, Sassetti CM. 2014. Subpolar addition of new cell wall is directed by DivIVA in mycobacteria. Proc Natl Acad Sci U S A 111:E3243–E3251. https://doi.org/10.1073/pnas.1402158111.
73. Joyce G, Williams KJ, Robb M, Noens E, Tizzano B, Shahrezaei V, Robertson BD. 2012. Cell division site placement and asymmetric growth in mycobacteria. PLoS One 7:e44582. https://doi.org/10.1371/journal.pone.0044582.
74. Santi I, Dhar N, Bousbaine D, Wakamoto Y, McKinney JD. 2013. Single-cell dynamics of the chromosome replication and cell division cycles in mycobacteria. Nat Commun 4:2470. https://doi.org/10.1038/ncomms3470.
75. Singh B, Nitharwal RG, Ramesh M, Pettersson BMF, Kirsebom LA, Dasgupta S. 2013. Asymmetric growth and division in *Mycobacterium* spp.: compensatory mechanisms for non-medial septa. Mol Microbiol 88:64–76. https://doi.org/10.1111/mmi.12169.
76. Rego EH, Audette RE, Rubin EJ. 2017. Deletion of a mycobacterial divisome factor collapses single-cell phenotypic heterogeneity. Nature 546:153–157. https://doi.org/10.1038/nature22361.
77. Hannebelle MTM, Ven JXY, Toniolo C, Eskandarian HA, Vuaridel-Thurre G, McKinney JD, Fantner GE. 2020. A biphasic growth model for cell pole elongation in mycobacteria. Nat Commun 11:452. https://doi.org/10.1038/s41467-019-14088-z.
78. Hett EC, Rubin EJ. 2008. Bacterial growth and cell division: a mycobacterial perspective. Microbiol Mol Biol Rev 72:126–156. https://doi.org/10.1128/MMBR.00028-07.
79. Egan AJF, Vollmer W. 2013. The physiology of bacterial cell division. Ann N Y Acad Sci 1277:8–28. https://doi.org/10.1111/j.1749-6632.2012.06818.x.
80. Chao MC, Kieser KJ, Minami S, Mavrici D, Aldridge BB, Fortune SM, Alber T, Rubin EJ. 2013. Protein complexes and proteolytic activation of the cell wall hydrolase RipA regulate septal resolution in mycobacteria. PLoS Pathog 9:e1003197. https://doi.org/10.1371/journal.ppat.1003197.
81. Takade A, Takeya K, Taniguchi H, Mizuguchi Y. 1983. Electron microscopic observations of cell division in *Mycobacterium vaccae* V1. J Gen Microbiol 129:2315–2320. https://doi.org/10.1099/00221287-129-7-2315.
82. Dahl JL. 2004. Electron microscopy analysis of *Mycobacterium tuberculosis* cell division. FEMS Microbiol Lett 240:15–20. https://doi.org/10.1016/j.femsle.2004.09.004.
83. Typas A, Banzhaf M, Gross CA, Vollmer W. 2011. From the regulation of peptidoglycan synthesis to bacterial growth and morphology. Nat Rev Microbiol 10:123–136. https://doi.org/10.1038/nrmicro2677.
84. Zhou X, Halladin DK, Theriot JA. 2016. Fast mechanically driven daughter cell separation is widespread in Actinobacteria. mBio 7:e00952-16. https://doi.org/10.1128/mBio.00952-16.
85. Zhou X, Halladin DK, Rojas ER, Koslover EF, Lee TK, Huang KC, Theriot JA. 2015. Mechanical crack propagation drives millisecond daughter cell separation in *Staphylococcus aureus*. Science 348:574–578. https://doi.org/10.1126/science.aaa1511.
86. Odermatt PD, Hannebelle MTM, Eskandarian HA, Nievergelt AP, McKinney JD, Fantner GE. 2020. Overlapping and essential roles for molecular and mechanical mechanisms in mycobacterial cell division. Nat Phys 16:57–62. https://doi.org/10.1038/s41567-019-0679-1.
87. Dufrêne YF. 2020. Together we are stronger: protein clustering at the nanoscale. ACS Nano 14:2561–2564. https://doi.org/10.1021/acsnano.0c01451.
88. Viljoen A, Mignolet J, Viela F, Mathelié-Guinlet M, Dufrêne YF. 2020. How microbes use force to control adhesion. J Bacteriol 202:e00125-20. https://doi.org/10.1128/JB.00125-20.
89. Heath GR, Scheuring S. 2018. High-speed AFM height spectroscopy reveals μs-dynamics of unlabeled biomolecules. Nat Commun 9:4983. https://doi.org/10.1038/s41467-018-07512-3.
90. Meister A, Gabi M, Behr P, Studer P, Vörös J, Niedermann P, Bitterli J, Polesel-Maris J, Liley M, Heinzelmann H, Zambelli T. 2009. FluidFM: combining atomic force microscopy and nanofluidics in a universal liquid delivery system for single cell applications and beyond. Nano Lett 9:2501–2507. https://doi.org/10.1021/nl901384x.
91. Guillaume-Gentil O, Potthoff E, Ossola D, Franz CM, Zambelli T, Vorholt JA. 2014. Force-controlled manipulation of single cells: from AFM to FluidFM. Trends Biotechnol 32:381–388. https://doi.org/10.1016/j.tibtech.2014.04.008.
92. Guillaume-Gentil O, Mittelviefhaus M, Dorwling-Carter L, Zambelli T, Vorholt JA. 2018. FluidFM applications in single-cell biology, p 325–354. *In* Delamarche E, Kaigala GV (ed), Open-space microfluidics. John Wiley & Sons, Inc, Hoboken, NJ.